JOURNAL GEOLOGICAL SOCIETY OF INDIA
Vol.80, December 2012, pp.855-868

Genetic Characteristics of the Gozecukuru As-Sb Deposits near Kutahya, Turkey

Fetullah Arik
Selçuk University, Engineering-Architecture Faculty, Department of Geological Engineering, 42031 Konya, Turkey
Email: farik@selcuk.edu.tr

Abstract: Gözeçukuru As-Sb-Pb-Zn mine is located 1.2 km NW of Sahin village and 22 km west of Kütahya in NW Turkey. The aim of this study is to explain the genetic characteristics of the As-Sb deposits by using multivariate statistical analysis methods. Low-grade metamorphic rocks of the upper Paleozoic Sahin Formation occur as the basement of the study area. Cenozoic volcano-sedimentary units (Tavsanli volcanites and Emet Formation) overlie the Sahin Formation unconformably. The mineralization occurs mainly as veins and partly as disseminations and fillings of interstices in the rhyodacitic and rhyolitic tuffs of Tavsanli Volcanics. Common primary ore minerals are stibnite, realgar, galena, sphalerite, pyrite and arsenopyrite, and secondary minerals are orpiment, senarmontite and valentinite. Barite is the dominant gangue mineral, with a small amount of quartz, calcite and dolomite. Average As, Sb, Pb, Zn and Ba concentrations in the samples from the study area are 6.04%, 4938 ppm, 4589 ppm, 1.17% and 10.36 % respectively. Three significant groups appear in the cluster analysis of ore samples. First group consists of Pb-Ag and Zn-Cd. The second group consists of Sb-Tl-Hg and As. The last group is the Ba-Sr. There are three significant factors in the factor analysis. First factor reflects the formation of primary sulphide minerals, the second factor represents the formation of low temperature sulphide and sulphosalt minerals and the last factor depicts interstices-filling mineralization. Average homogenization temperature of the fluid inclusion in barites is 221 ºC. Geological, petrographical and geochemical data suggest that the Gözeçukuru As-Sb deposit was formed under epithermal conditions.

Keywords: Epithermal deposit, Kütahya, Cluster analysis, Factor analysis, Gözeçukuru, Turkey.

INTRODUCTION

Epithermal ore deposits have become important nowadays. Some of them have typical genetic characteristics and contain precious metals in significant amounts. Although the Gözeçukuru As-Sb deposit is relatively small, it is important for its geochemical and geological characteristics. The deposit covers an area of 2.1 km^2, located among the Tavukkiran and Sigiregregi Hills, and Egen and Degirmendere Creeks, 1.2 km NW of Sahin Village and 22 km west of Kütahya (Fig. 1).

There are many Sb, As, Ag, Pb, Zn and Cu enrichments related to the Cenozoic volcanic activities near the study area (NW Kütahya). Some of these enrichments attained minable reserves. Many wells and galleries, hollow concavities and splitting, belonging to old mining activities, are present at the Aktepe silver deposit (northern boundary of the study area), Sigiregregi lead-zinc deposits (eastern boundary of the study area) and an open-pit mine in the Gözeçukuru area. An average of 3900 ± 85 years by ^{14}C isotopic studies of the coal and burnt firewood, collected from the old galleries, indicate that mining activities in this area dates back to the old Bronze Age (Yigitgüden, 1984). In addition, different researchers found many artifacts such as pots, vessels, picks, shovels, hatchets and knives made of soil, bronze, gold and silver (Vicil, 1982; Yigitgüden, 1984; Arik, 2002).

The reserve of the Gözeçukuru Sb-As-Pb-Zn deposit was calculated as 277.2 mt (Arik, 2002). Surface samples have an average 0.49% Sb and the antimony reserve of the deposit is 0.135 mt. Pb reserve of the deposit is 1.27 mt while Zn reserve is 3.23 mt. In addition the Ag, Cd and Tl reserves are 22176 t, 103395 t and 16354 t respectively (Arik, 2002). Antimony and thallium have been mined from the Gözeçukuru ore deposits in 1960's.

The Gözeçukuru Mine and its vicinity were studied by a number of researchers (Ildiz, 1967; Erdogan, 1971; Akyol, 1975; Ercan, 1979, 1982; Gün et al. 1979; Ünsal and Koçak, 1981; Vicil, 1982; Yigitgüden, 1984; Ercan et al. 1985; Bas, 1986, 1987; Kafkas, 1994; Karabas, 1997; Çelik and Kerey, 1999; Sengüler and Sonel, 1999; Arik, 2002, 2008; Arik and Temur, 2003; Arik and Nalbatçilar, 2004; Arik et al. 2008). All these researchers indicate that the basement of

the study area consists of low-grade metamorphic rocks of the Carboniferous–Permian Sahin Formation. This formation is overlain unconformably by a Tertiary volcano-sedimentary sequence (rhyolitic and rhyodacitic tuffs of the Tavsanli volcanics, and limestone and dolomitic limestones of the Emet Formation). Researchers who studied the ore deposits in the study area (e.g., Ziegler, 1960; Vicil, 1982; Yigitgüden, 1984; Arik, 2002, 2008) pointed to the presence of As-Sb-Pb-Zn enriched zones in the area.

The aim of the present study is to elucidate the genetic characteristics of the As-Sb-Pb-Zn deposits by using multivariate statistical analysis method based on stratigraphic position and geological, mineralogical and petrographical features.

SAMPLING AND ANALYTICAL METHODS

The study area was visited in 2002–2004 and 2007 to check different formation boundaries and to collect samples from ore-host rocks and wall rocks. Forty seven samples consisting of lead, zinc, antimony and arsenic sulphide and sulphosalts, such as galena, sphalerite, stibnite, realgar, tetrahedrite, tennantite, argentite, pyrargyrite, praustite pyrostilpnite, stephanite, andorite, cinnabar, enargite, boulangerite and bournonite, and barite were randomly collected from the rhyolitic and rhyodacitic tuffs of the Tavþanlý Volcanics (GC) in the Gözeçukuru Mine and near its vicinity (Fig. 1, Table 1). A total of seven wall-rock samples, three from low-grade metamorphic rocks of the Sahin Formation (GS); four from limestone, silicified limestone and dolomitic limestone of the Emet Formation (GL) were also collected to obtain their characteristics and to determine secondary dispersion in the ore deposits (Fig. 1, Table 1).

All rock and ore samples were dried at room temperature. Mineralogical-petrographic features of thin and polished sections of the rock and ore samples were studied in the Petrography Laboratory of the Selçuk University's Geological Engineering Department (Konya-Turkey).

Crushed and sieved rock samples were chemically analyzed at ACME Analytical Laboratories Ltd., Vancouver, Canada, by Inductively Coupled Plasma–Emission Spectrometry (ICP-ES) for major elements and by Inductively Coupled Plasma–Mass Spectrometry (ICP-MS) for the heavy metal content (Ag, As, Pb, Zn, Sb, Cu, Sr, Cd, Hg). Wall rocks and hard ore samples were jaw-crushed to 70%, passing 10 mesh (2 mm), and a 250 g aliquot was riffle-split and pulverized to 95%, passing 150 mesh (100 μm) in a mild-steel ring-and-puck mill. A 0.2 g sample aliquot was weighed in a graphite crucible and mixed with 1.5 g of $LiBO_2/Li_2B_4O_7$ flux. The flux/sample charge was heated in a muffle furnace for 30 minutes at 980 °C. The cooled bead was dissolved in 100 ml of 5% HNO_3 (ACS grade nitric acid in demineralised water). An aliquot of the solution was poured into a polypropylene test tube. Calibration standards, verification standards and reagent blanks were included in the sample sequence. Sulphide samples exceeding the upper detection limits of this method were re-analyzed. In the re-analyzing process a 1.0 g sample was digested in 100 ml of aqua regia ($HCl-HNO_3-H_2O$), and sample solutions were analyzed by ICP-ES.

All geochemical data for the rock and ore samples were evaluated by basic and multivariate analysis methods such as normal and logarithmic classification and Student's t test, correlation coefficients, simple regression, scatter diagrams and cluster and factor analyses. Seven ore samples were removed while doing the multivariate analysis, since their chemical characters did not fit to the normal distribution. Thus, all statistical analysis was performed by using outliers' free data.

GEOLOGICAL SETTING AND STRATIGRAPHY

The As-Sb mineralization formed within the low-grade metamorphic rocks of the Sahin Formation, rhyolitic and rhyodacitic tuffs of the Tavsanli volcanics, and limestone and dolomitic limestones of the Emet Formation. The ore deposit exhibits lens-shape with long axis trending NE-SW (Fig. 1).

The Sahin Formation comprises pink, green, red and beige colored low-grade metamorphic phyllite, quartz schist, mica schist, talc schist, calc-schist, graphite schist, chlorite schist, chloritoid schist, meta-sandstone, meta-conglomerate, and meta-carbonate as well as quartzite interbeds and lenses. The Sahin Formation was deposited during Carboniferous–Permian time in a shore environment favourable for detrital and carbonate deposition.

The Tavsanli volcanics consist of mainly agglomerate, fine-grained vitric tuffs, fine-grained crystalline tuffs, lapilli-sized tuff and ponza, which are rhyolitic and rhyodacitic in composition and comprise rock fragments in large amount. The rhyolitic tuffs are generally green, yellow and brown and include lens-shaped clay and sandstone interbeds as well as lapilli and ponza fragments; the thickness of these tuffs attains several tens of meters. The rhyodacitic tuffs comprise principally quartz, plagioclase, biotite, alkali feldspar and opaque minerals (galena, sphalerite, pyrite, stibnite, Mn oxide and chalcopyrite) and chalcedony, witherite and cerussite in places. The Tavsanli volcanics overlie the Sahin Formation uncomformably and in turn are

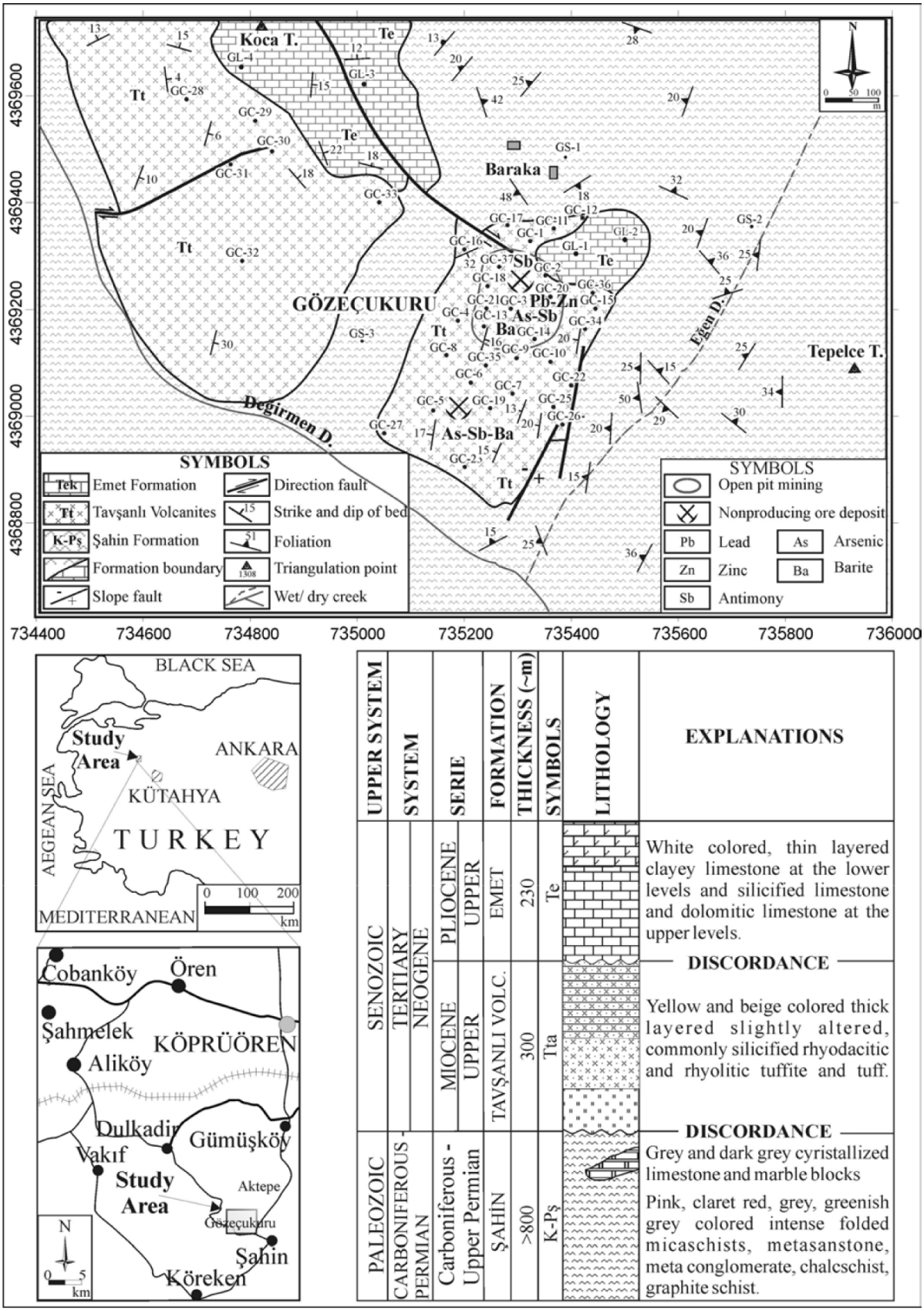

Fig. 1. Location and geological map and stratigraphic column of the study area (modified from Yaldiz, 2007, and Arik, 2008).

Table 1. Sample description and locations (GC: Rhyolitic and rhyodacitic tuffs of the Tavþanlý Volcanites, GL: Silicified limestone and dolomitic limestones of the Emet formation, GS: Low metamorphic detrital rocks of the ªahin Formation)

Code	*Sample description*	GPS DATA	
	Rhyolitic and rhyodacitic tuffs	***X***	***Y***
GC-1	Rhyodacitic tuff (argentite,sphalerite and realgar mineralization)	735326	4369337
GC-2	Rhyodacitic tuff (antimonite, orpiment and realgar mineralization)	735361	4369267
GC-3	Rhyodacitic tuff (orpiment, valentinite mineralization)	735287	4369200
GC-4	Rhyodacitic tuff (orpiment and valentinite mineralization)	735185	4369180
GC-5	Rhyolitic tuff (realgar, orpiment and barite mineralization)	735154	4369011
GC-6	Rhyolitic tuff (barite mineralization)	735215	4369061
GC-7	Rhyolitic tuff (barite mineralization)	735289	4369049
GC-8	Silicified rock (realgar mineralization)	735185	4369177
GC-9	Silicified rhyodacitic (realgar, orpiment and antimonite mineralization)	735296	4369109
GC-10	Silicified rhoyodacitic tuff (realgar and antimonite mineralization)	735359	4369102
GC-11	Siliceous rhyodacitic tuff (galena, sphalerite, realgar and barite mineralization)	735372	4369351
GC-12	Siliceous rhyodacitic tuff (galena, sphalerite, realgar and barite mineralization)	735421	4369380
GC-13	Rhyolitic tuff (realgar, antimoniteand barite mineralization)	735222	4369180
GC-14	Rhyodacitic tuff (sphalerite, galena, realgar and barite mineralization)	735278	4369161
GC-15	Rhyolitic tuff (Ba, As, Pb, Zn mineralization)	735412	4369202
GC-16	Rhyolitic tuff (Ba, Zn, Pb, As mineralization)	735203	4369315
GC-17	Siliceous rhyodacitic tuff (As, Sb, Pb, Zn, Ba mineralization)	735274	4369354
GC-18	Siliceous rhyodacitic tuff (Zn, Pb, Sb, As, Ba mineralization)	735247	4369244
GC-19	Siliceous Rhyolitic tuff (Sb, As, Ba mineralization)	735253	4369015
GC-20	Rhyodacitic tuff (Zn, Sb, As, Pb, Ba mineralization)	735362	4369222
GC-21	Siliceous rhyodacitic tuff (Zn, Pb, Ba mineralization)	734242	4369197
GC-22	Siliceous rhyodacitic tuff (As, Sb, Pb, Zn, Ba mineralization)	734398	4369652
GC-23	Siliceous rhyodacitic tuff (As, Ba mineralization)	735202	4368905
GC-24	Siliceous rhyodacitic tuff (As, Pb, Zn, Ba mineralization)	735256	4369108
GC-25	Siliceous rhyodacitic tuff (Pb, Zn, As, Ba, Fe mineralization)	735368	4369022
GC-26	Siliceous rhyodacitic tuff (Pb, Zn, As, Ba mineralization)	735388	4368983
GC-28	Siliceous rhyodacitic tuff (Zn, Pb, Ba)	734679	4369602
GC-29	Siliceous rhyodacitic tuff (Pb, Zn, Ba, Sb, Fe mineralization)	734814	4369548
GC-30	Siliceous rhyodacitic tuff (Zn, Pb, Sb, As mineralization)	734842	4369494
GC-31	Sliceous rhyodacitic tuff (Pb, Zn, As, Sb, Ba mineralization)	734765	4369472
GC-32	Siliceous rhyolitic tuff (As, Ba mineralization)	734781	4369296
GC-27	Rhyolitic tuff with barite	735052	4368977
GC-33	Siliceous rhyolitic tuff (As, Ba mineralization)	735041	4369400
GC-34	Siliceous rhyodacitic tuff (Pb, Zn, As, Ba mineralization)	735458	4369162
GC-35	Siliceous rhyolitic tuff (Ba, As, Sb, Pb, Zn mineralization)	735386	4369242
GC-36	Siliceous rhyolitic tuff (As, Sb, Ba, Zn, Pb, Fe mineralization)	735440	4369232
GC-37	Siliceous rhyodacitic tuff (As, Ba, Zn, Pb, Fe mineralization)	735272	4369280
Limestone samples			
GL-1	Siliceous dolomitic limestone	735403	4369301
GL-2	Siliceous limestone	735472	4369321
GL-3	Siliceous dolomitic limestone	735003	4369616
GL-4	Siliceous dolomitic limestone	734777	4369658
Low metamorphic rock samples			
GS-1	Metasandstone	735403	4369482
GS-2	Metasandstone	735716	4369355
GS-3	Micaschist	735003	4369120

overlain by the Pliocene Emet Formation.

The Emet Formation is represented principally by clayey limestone, limestone, siliceous limestone and dolomitic limestone. Mainly horizontal and near-horizontal beds are represented by thin- and medium-layered white and beige limestone, thin clayey-limestone layers and porous dolomitic limestone. Limestone is intensely fractured, some of the fractures are filled with barite, quartz and with minor amount (<% 1) of stibnite and galena. Dolomite and dolomitic limestone consist of fine-grained, dark-colored cryptocrystalline dolomite fragments and light-colored microcrystalline dolomite cement. The dolomite is also intensely fractured and has a lot of interstices and some of them are filled by coarsely crystalline barite and quartz.

ORE TYPES AND MINERAL PARAGENESIS

The As-Sb-Pb-Zn mineralization occurs mainly in the rhyodacitic and rhyolitic tuffs of the Tavsanli volcanics. Some weakly mineralized veins are present in the low-grade metamorphic rocks of the Sahin Formation, and limestone and dolomitic limestone of the Emet Formation. The ores exhibit lens-shaped geometry with long axis oriented NW-SE. The mineralization can be divided into two separate

phases: primary and secondary mineralization. In addition, mineral paragenesis can be divided into three subgroups: primary ore minerals, secondary ore minerals and gangue minerals (Table 1, Arik, 2002; Yaldiz, 2007; Arik, 2008).

Primary ore minerals are stibnite, realgar, galena, sphalerite, tetrahedrite-tennantite, hematite, pyrite, arsenopyrite, argentite, pyrargyrite, praustite, pyrostilpnite, stephanite, andorite, enargite, boulangerite and bournonite in decreasing order (Figs. 2 and 3).

Secondary ore minerals are orpiment, cerussite, smithsonite, hydrozincite, chalcocite, covellite, malachite, azurite, native silver, achantite, As oxide, Mn oxide and antimony ocher (valentinite, senarmontite). Common gangue minerals are barite, quartz, calcite and dolomite (Figs. 2 and 3).

Three-ore types are found in the Gözeçukuru mine. These are vein, dissemination and interstice and cavity fillings. Vein-type mineralizations are of two types: stibnite and stibnite + realgar + orpiment + barite veins and veinlets. Stibnites are altered by the atmospheric conditions near the surface and some pseudomorph antimony oxides are formed in the altered interstices of primary stibnites (Arik, 2008). In addition, lesser amounts of galena + sphalerite, galena + sphalerite + barite, galena + barite + quartz veins and veinlets are noted. Cyrstalline galena-barite-quartz veins have fine cyrstallized galenas and minor amounts of barite and quartz. Outer zones of some galena ore show alteration . Cerussite, some fine crystallized isometric argentite and tetrahedrite crystals are found in the altered zones. In addition, some veins have only quartz or barite (Figs. 2 and 3). Vein-type mineralizations are located commonly in the rhyodacitic tuffs of Tavsanli volcanics. Rhyolitic tuffs, mica schists and limestones also have ore veins and veinlets in decreasing order. There are arsenic (realgar and orpiment) and antimony (stibnite and antimony ocher) enrichments in the contact zone between the tuffs of Tavsanli volcanics and limestones of the Emet Formation (Figs. 2 and 3).

Stibnite – realgar – orpiment - barite enrichments were observed in the abandoned open pit mine area. The ore is light yellow to light greenish-gray in color and very soft. Stibnite + barite veins are the most common vein type occurring in the siliceous rhyodacitic tuffs (Arik, 2008). Unaltered stibnite crystals were observed among the senarmontite, valentinite and barite crystals in the barite rich samples. Cavity and interstice filling textures were noted in the unaltered samples (Fig. 2).

Disseminated ore types occur in the rhyolitic and rhyodacitic tuffs of the Tavsanli volcanics, and are represented by stibnite, realgar and minor galena and sphalerite. Tuffs have abundant pores through which mineralized solutions circulated in these rocks. Interstice-filling ore formed as a late phase of principal mineralization and is composed of realgar, orpiment and gangue minerals, such as, barite and little quartz, dolomite, calcite and chalcedony (Fig 3; Table 1). All ore types are altered near the surface, resulting in some secondary sulphide minerals (Arik, 2002; Arik, 2008). Some oxide, carbonate minerals such as senarmontite, valentinite, cerussite, hydrozincite, smithsonite, chalcocite, covellite, malachite, azurite, native silver and achantite were formed as a result of the decomposition of primary ore minerals.

Common alteration zones were formed by intermittent volcanic activity since the middle Miocene, which caused argillic-alteration of volcanic rocks and silicification of limestones.

RESULTS AND DISCUSSION

The results of chemical analyses of rhyolitic and rhyodacitic tuffs containing ore are given in Tables 2 and 3. Mean SiO_2, Al_2O_3, Fe_2O_3, MgO, CaO, TiO_2 and MnO of rhyolitic and rhyodacitic samples hosting mineralization from the Gözeçukuru Mine are 44.97%, 2.30%, 4.85%, 0.15%, 0.52%, 0.08% and 0.44%, respectively (Table 2). Trace element contents of ore samples, such as, Pb, Zn, As, Sb, Cd, Ag, Hg, Tl, Ba and Sr—are (Table 3) higher than those of mean values in the earth's crust (Gümüs, 1998). According to Student's t test, the majority of samples contain significant elemental contents at the 95% confidence level (Tables 2 and 3).

On the basis of the statistical-analysis average, the As content of ore samples is 6.04%, and the expected As of the main mass of the samples ranges from 3.4% to 8.7%. The arsenic content is derived from realgar, arsenopyrite and tetrahedrite from primary mineralization, and native As and orpiment from secondary enrichment of Gözeçukuru mineralization. Arsenic in the study area was fixed during later phases of primary mineralization. Primary As minerals were easily altered by weathering under surface and near-surface conditions. As was redeposited as native As or, rather commonly, as orpiment, and is present in a wide area around the Gözeçukuru Mine (Arik, 2002).

The average Sb content in the Gozeçukuru Mine is 4938 ppm, and the estimated Sb range in the mine is 3138–6738 ppm. Antimony is present as stibnite and is the most widespread ore mineral in the study area. Many stibnite crystals have been altered to Sb oxide minerals such as valentinite and senarmontite at the surface and near surface. Several centimeter-sized stibnite crystals in veins and pores of the wall rocks are needle shaped and granular. Some

Table 2. Major elements analysis results (%) and statistical summaries of the rhyolitic and rhyodacitic tuff samples (tc: calculated t value. μ_l: Lower limit Interval of the difference with 95% confidence. μ_u Upper limit Interval of the difference with 95% confidence)

Sample No.	SiO_2	Al_2O_3	Fe_2O_3	MgO	CaO	Na_2O	K_2O	TiO_2	P_2O_5	MnO	Cr_2O_3
GC-1	2.05	0.07	0.15	0.01	0.05	0.02	0.04	0.01	0.04	0.35	0.001
GC-2	40.08	1.98	1.01	0.03	0.09	0.06	1.07	0.15	0.01	0.01	0.002
GC-3	59.52	3.72	1.44	0.05	0.07	0.09	2.16	0.21	0.01	0.01	0.003
GC-4	66.99	4.11	2.50	0.05	0.07	0.10	2.46	0.25	0.02	0.01	0.004
GC-5	13.95	1.97	1.44	0.02	0.01	0.03	0.25	0.13	0.06	0.01	0.003
GC-6	0.99	0.20	0.28	0.01	0.08	0.01	0.04	0.02	0.01	0.05	0.002
GC-7	5.60	0.79	0.71	0.01	0.01	0.01	0.11	0.05	0.01	0.01	0.003
GC-8	74.85	8.63	1.80	0.11	0.18	0.25	6.64	0.22	0.03	0.03	0.064
GC-9	22.24	1.49	0.66	0.59	1.42	0.05	0.77	0.09	0.01	0.01	0.003
GC-10	62.12	3.92	1.67	0.06	0.09	0.09	2.29	0.23	0.02	0.01	0.004
GC-11	56.20	3.30	8.15	0.15	0.34	0.02	1.95	0.04	0.15	1.53	0.009
GC-12	62.30	4.35	6.25	0.10	0.43	0.05	1.90	0.08	0.15	1.07	0.007
GC-13	8.45	3.40	13.00	0.04	1.45	0.08	1.35	0.12	0.15	0.00	0.001
GC-14	6.75	2.30	1.50	0.20	0.90	0.07	0.08	0.04	0.20	1.31	0.200
GC-15	36.55	1.60	10.20	0.07	1.95	0.05	1.35	0.10	0.20	0.04	0.200
GC-16	17.10	1.34	13.20	0.10	0.62	0.04	0.01	0.07	1.00	0.00	0.002
GC-17	19.75	2.56	12.00	0.15	0.55	0.05	0.03	0.03	0.70	0.01	0.004
GC-18	65.60	2.50	1.27	0.10	0.34	0.03	1.55	0.05	0.03	0.60	0.001
GC-19	71.30	2.80	1.45	0.28	0.65	0.03	1.87	0.01	0.01	0.38	0.003
GC-20	45.73	8.82	2.91	0.48	0.80	0.09	0.20	0.20	1.22	0.02	0.002
GC-21	61.04	0.36	5.50	0.14	0.71	0.04	0.08	0.02	0.11	0.09	0.002
GC-22	27.18	0.73	0.89	0.04	0.28	0.03	0.09	0.02	0.03	0.33	0.001
GC-23	63.38	2.04	0.72	0.09	0.22	0.28	0.46	0.04	0.12	0.17	0.018
GC-24	81.72	2.45	0.56	0.05	0.10	0.09	0.33	0.04	0.12	0.17	0.008
GC-25	54.88	1.33	14.73	0.09	0.08	0.02	0.04	0.01	0.24	0.53	0.002
GC-26	46.18	3.18	6.79	0.53	1.50	0.04	0.57	0.11	0.23	2.65	0.008
GC-28	72.30	2.10	0.29	0.04	0.16	0.04	2.45	0.08	0.01	0.13	0.005
GC-29	36.61	0.41	28.89	0.04	0.10	0.02	0.15	0.02	0.10	3.58	0.012
GC-30	68.70	3.40	1.61	0.02	0.15	0.03	2.60	0.01	0.01	0.13	0.004
GC-31	17.03	0.46	0.98	0.11	1.16	0.01	0.70	0.01	0.07	0.31	0.002
GC-32	32.50	1.30	1.19	0.06	0.21	0.05	0.70	0.20	0.02	0.20	0.004
GC-27	58.34	1.24	1.24	0.35	0.88	0.09	0.38	0.06	0.10	0.37	0.019
GC-33	70.05	2.81	0.84	0.39	0.78	0.05	1.23	0.03	0.04	0.07	0.024
GC-34	72.41	0.29	1.41	0.35	0.65	0.04	0.06	0.02	0.07	0.99	0.018
GC-35	54.45	1.50	9.70	0.20	0.30	0.06	0.60	0.14	0.06	0.70	0.003
GC-36	52.26	0.07	15.90	0.42	0.65	0.04	0.09	0.02	0.20	0.29	0.005
GC-37	56.54	1.65	6.25	0.05	1.32	0.20	0.45	0.02	0.21	0.18	0.013
N	37	37	37	37	37	37	37	37	37	37	37
Mean	44.97	2.30	4.84	0.15	0.52	0.06	1.00	0.08	0.16	0.44	0.018
Std. Deviation	24.18	1.97	6.21	0.16	0.51	0.06	1.27	0.07	0.26	0.76	0.034
Std. Error Mean	3.98	0.32	1.02	0.03	0.08	0.01	0.21	0.01	0.04	0.12	0.006
t_c	11.31	7.10	4.74	5.75	6.28	6.39	4.79	6.61	3.60	3.54	1.924
μ_l	36.90	1.64	2.77	0.10	0.35	0.04	0.58	0.06	0.07	0.19	0.000
μ_u	53.03	2.96	6.91	0.20	0.69	0.08	1.43	0.10	0.24	0.70	0.020

stibnite skeletons are filled with secondary antimony minerals. Stibnite mineralization occurred in the late phase of the main mineralization, reflecting a low-temperature hydrothermal stage.

The mean Zn content of the ore samples is 11662 ppm, ranging from 7528 to 15796 ppm. The zinc is derived from primary sphalerite, tetrahedrite and secondary smithsonite. Sphalerite, which is a primary Zn mineral, may easily alter under surface conditions and transform into smithsonite. For that reason, smithsonite was observed more often than sphalerite in the study area.

The mean Pb content is 4589 ppm, ranging from 100 to 14830 ppm. The lead is derived from primary galena and tetrahedrite and from secondary cerussite and minor anglesite. Galena is a typical hydrothermal mineral and occurs in many veins with fine crystalline textures. The surfaces of some galena are altered to secondary Ag minerals, such as, argentite and freibergite.

Analyzed samples have 88 ppm Ag in average, ranging from 0.1 to 453 ppm. The silver is sourced from argentite and Ag-rich tetrahedrite (freibergite) around the altered galenas. In addition, minor amount of Ag is derived from tennantite, pyrargyrite, praustite, pyrostilpnite, stephanite, andorite, enargite, boulangerite, bournonite, native Ag and achanthite in the mineralized zone. Especially siliceous rhyodacitic tuffs have more Ag than those of the other units.

The mean Cd content of the samples is 59 ppm, ranging from 2 to 200 ppm. The presence of cadmium depends on

Table 3. Trace elements analysis results and statistical summaries of the rhyolitic and rhyodacitic tuff samples (tc: calculated t value. μ_l: Lower limit Interval of the difference with 95% Confidence. μ_u Upper limit Interval of the difference with 95% confidence)

Sample No.	Ni	Cu	Pb	Zn	As	Cd	Sb	Ag	Hg	Tl	Ba	Sr	Zr
GC-1	11.0	254.7	4388.9	47600.0	24000.0	271.7	418.1	141.0	9.5	100.0	322722.0	5356.9	2.3
GC-2	10.1	8.5	100.0	400.0	267000.0	10.0	6100.0	2.0	39.5	600.0	13858.3	332.3	33.9
GC-3	19.2	23.5	200.0	900.0	140000.0	10.0	3750.0	2.4	52.1	600.0	18346.9	457.9	46.1
GC-4	35.0	13.5	100.0	300.0	97000.0	10.0	3300.0	2.0	39.4	800.0	8162.0	226.9	67.2
GC-5	4.0	26.2	4691.7	229.0	2113.3	20.8	957.4	1.4	20.2	89.0	266028.6	2851.3	26.1
GC-6	12.1	4.4	696.2	341.0	1300.0	29.9	5030.0	0.1	10.0	400.0	219563.0	5712.1	4.5
GC-7	9.0	13.8	760.0	101.0	508.2	13.0	436.7	0.6	13.6	39.9	233553.2	3696.2	9.9
GC-8	35.9	100.0	200.0	204.0	17700.0	6.6	680.0	2.0	7.1	100.0	13050.8	397.6	121.0
GC-9	11.4	26.6	231.3	200.0	388000.0	2.4	4610.0	1.4	19.3	300.0	6507.2	199.8	21.5
GC-10	25.9	17.9	118.0	482.0	133000.0	10.0	3210.0	0.9	42.3	600.0	12775.9	351.8	55.8
GC-11	70.0	400.0	14830.0	30300.0	10200.0	200.0	2767.3	453.0	45.4	70.0	118000.0	700.0	65.4
GC-12	5.0	300.0	11000.0	29000.0	17300.0	200.0	2504.3	245.0	10.3	40.0	71600.0	2100.0	40.0
GC-13	200.0	40.0	1250.0	3300.0	81700.0	7.0	15100.0	20.0	100.0	1200.0	326700.0	2000.0	70.0
GC-14	40.0	100.0	13400.0	40700.0	28800.0	200.0	736.0	240.0	11.6	40.0	473500.0	2000.0	70.0
GC-15	30.0	4.0	5800.0	1450.0	8940.0	5.0	854.0	120.0	10.0	40.0	135500.0	1500.0	200.0
GC-16	70.0	40.0	2500.0	6500.0	4650.0	2.0	758.0	1.0	13.5	800.0	143000.0	200.0	40.0
GC-17	100.0	30.0	3240.0	9450.0	73400.0	10.0	12300.0	90.0	12.4	1000.0	125500.0	1500.0	34.0
GC-18	25.0	180.0	8350.0	19150.0	124000.0	145.0	11250.0	120.0	110.0	900.0	11120.0	150.0	45.0
GC-19	30.0	30.0	790.0	3150.0	121000.0	20.0	11260.0	1.0	80.0	800.0	21700.0	245.0	4.0
GC-20	30.4	36.1	5511.1	15200.0	87100.0	30.0	13300.0	110.0	120.0	88.9	9641.7	753.1	111.4
GC-21	58.4	318.4	6844.4	14500.0	17200.0	30.0	3955.6	135.0	142.2	30.0	33001.8	588.0	11.1
GC-22	11.7	35.0	2488.9	7771.0	10600.0	7.0	2673.0	60.0	19.9	47.4	180407.6	2071.6	10.8
GC-23	6.6	177.8	1455.0	3778.0	11500.0	5.0	2013.3	20.0	53.3	88.9	91566.0	296.0	87.8
GC-24	6.8	430.2	8577.8	16900.0	21300.0	83.0	2951.1	130.0	17.8	88.9	19711.0	63.3	50.8
GC-25	9.7	74.0	10100.0	25200.0	6400.0	100.0	260.0	135.0	10.0	88.9	57368.3	276.9	5.8
GC-26	62.8	236.8	12800.0	30900.0	16300.0	100.0	5924.5	120.0	8.9	177.8	65949.1	773.8	41.5
GC-28	5.0	495.0	4500.0	15400.0	5650.0	120.0	50.0	95.0	5.0	10.0	21900.0	645.0	34.0
GC-29	20.9	44.8	5422.2	16700.0	3859.3	10.0	100.0	105.0	35.6	7.6	78018.3	333.0	10.3
GC-30	15.0	25.0	5320.0	11600.0	122000.0	110.0	15800.0	110.0	120.0	1000.0	420.0	75.0	32.0
GC-31	70.0	70.0	9050.0	28500.0	52500.0	200.0	3200.0	180.0	40.0	700.0	6500.0	270.0	5.0
GC-32	10.0	550.0	3600.0	4170.0	11200.0	10.0	507.8	90.0	2.0	30.0	20500.0	495.0	164.6
GC-27	23.7	39.1	1078.3	2568.0	2162.0	29.0	104.4	20.0	2.0	4.6	11333.2	208.0	26.1
GC-33	7.4	31.2	1155.6	3644.0	25700.0	20.0	1080.0	20.0	8.0	35.3	78421.3	1087.8	11.9
GC-34	5.4	53.7	10900.0	16500.0	32800.0	120.1	364.4	235.0	9.0	88.9	146511.0	2527.8	9.3
GC-35	20.0	1160.0	3000.0	8750.0	78000.0	10.0	13400.0	85.0	200.0	1000.0	201000.0	1000.0	33.0
GC-36	30.0	10.0	2600.0	7800.0	132000.0	20.0	18100.0	80.0	19.6	900.0	39000.0	400.0	35.0
GC-37	40.0	40.0	2760.0	7850.0	58000.0	10.0	12900.0	80.0	120.0	900.0	231500.0	2000.0	35.8
N	37	37	37	37	37	37	37	37	37	37	37	37	37
Mean	31.8	147.0	4589.4	11661.8	60402.2	59.1	4938.0	87.9	42.7	373.1	103619.9	1184.9	45.2
Std. Deviation	36.7	227.6	4244.0	12399.5	80478.0	74.5	5399.7	95.2	48.1	393.5	113888.8	1384.2	44.2
Std. Error Mean	6.0	37.4	697.7	2038.5	13230.5	12.2	887.7	15.7	7.9	64.7	18723.2	227.6	7.3
t_c	5.3	3.9	6.6	5.7	4.6	4.8	5.6	5.6	5.4	5.8	5.5	5.2	6.2
μ_l	19.6	71.1	3174.4	7527.6	33569.6	34.3	3137.7	56.2	26.7	241.9	65647.5	723.4	30.5
μ_u	44.0	222.9	6004.5	15796.1	87234.9	84.0	6738.3	119.7	58.7	504.3	141592.3	1646.5	59.9

the zinc in the Zn-rich minerals such as sphalerite, fahlore and smithsonite. Siliceous rhyodacitic tuffs have more sphalerite and Cd than other units.

The mean Ba sample content is 10.4%, ranging from 6.6% to 14.2%. Some veins contain only barite. On the basis of the high barite content, the deposit itself can be considered as a barite deposit. The average contents of the other elements—Cu, Cd, Ag, Hg, Tl and Sr—are 147, 59, 88, 43, 373 and 1185 ppm, respectively. A high Sr content is derived from the barite, whereas the Cd is related to the occurrence of Zn.

The chemical analyses of four poorly mineralized calcareous rocks of Emet Formation and three low grade metamorphic rocks of the Sahin Formation indicate the presence of minor amounts of Ag, Pb, Zn, Sb and the other elements. While ore deposition developed mainly in the rhyolitic and rhyodacitic tuffs of Tavsanli volcanics, the other units, which are located in the lower and upper boundaries of ore mineralization, have dispersed mineralization.

Correlation and regression analyses of the outliers free data of 37 ore samples were carried out, using multivariate statistical methods. Although trace elements have strong and very strong correlation coefficients with each other, major oxides don not show any significant correlations except in a few oxide pairs, such as, SiO_2- K_2O, SiO_2-TiO_2 (Table 4). For instance, Pb has very strong correlation coefficient with Ag and strong positive correlation coefficients with respect to Zn and Cd. In addition, Zn has very strong positive correlation with respect to Cd and strong positive correlation

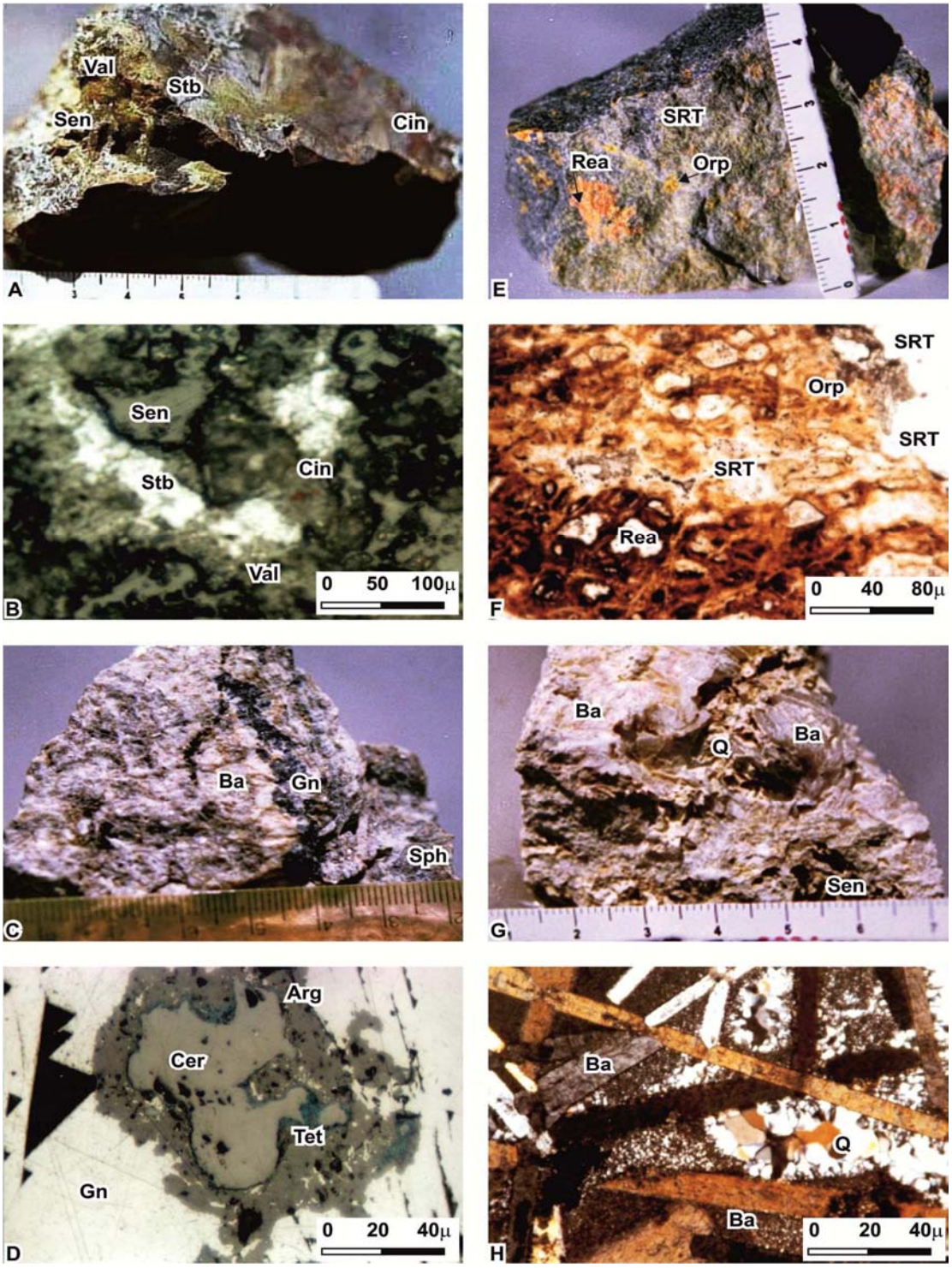

Fig.2. Some primary, secondary and gangue minerals in the vein type mineralization of the Gözeçukuru deposit; (A) Stibnite (Stb), cinnabar (Cin), senarmontite (Sen) and valentinite (Val) in the siliceous rhyodacitic tuffs, (B) Stibnite (Stb), cinnabar (Cin), senarmontite (Sen) and valentinite (Val) in the siliceous rhyodacitic tuffs (polished section, X nicols), (C) Fine cyristallized galena (Gn), sphalerite (Sph) and barite veinlet in the Siliceous Rhyodacitic tuffs, (D) Cerussite (Cer), tetrahedrite (Tet) and argentite along the outer border of a galena (Gn) (polished section, X nicols), E) Orpiment (Orp) and realgar (Rea) in the rhyodacitic tuffs (SRT), (F) Orpiment (Orp) and realgar (Rea) in the siliceous rhyolitic tuffs (SRT) (Thin section, //N), (G) Idiomorphic barite (Ba) and quartz (Q) in a barite-quartz vein, H) Idiomorphic barite (Ba) and quartz (Q) in a barite-quartz vein (thin section, X nicols)

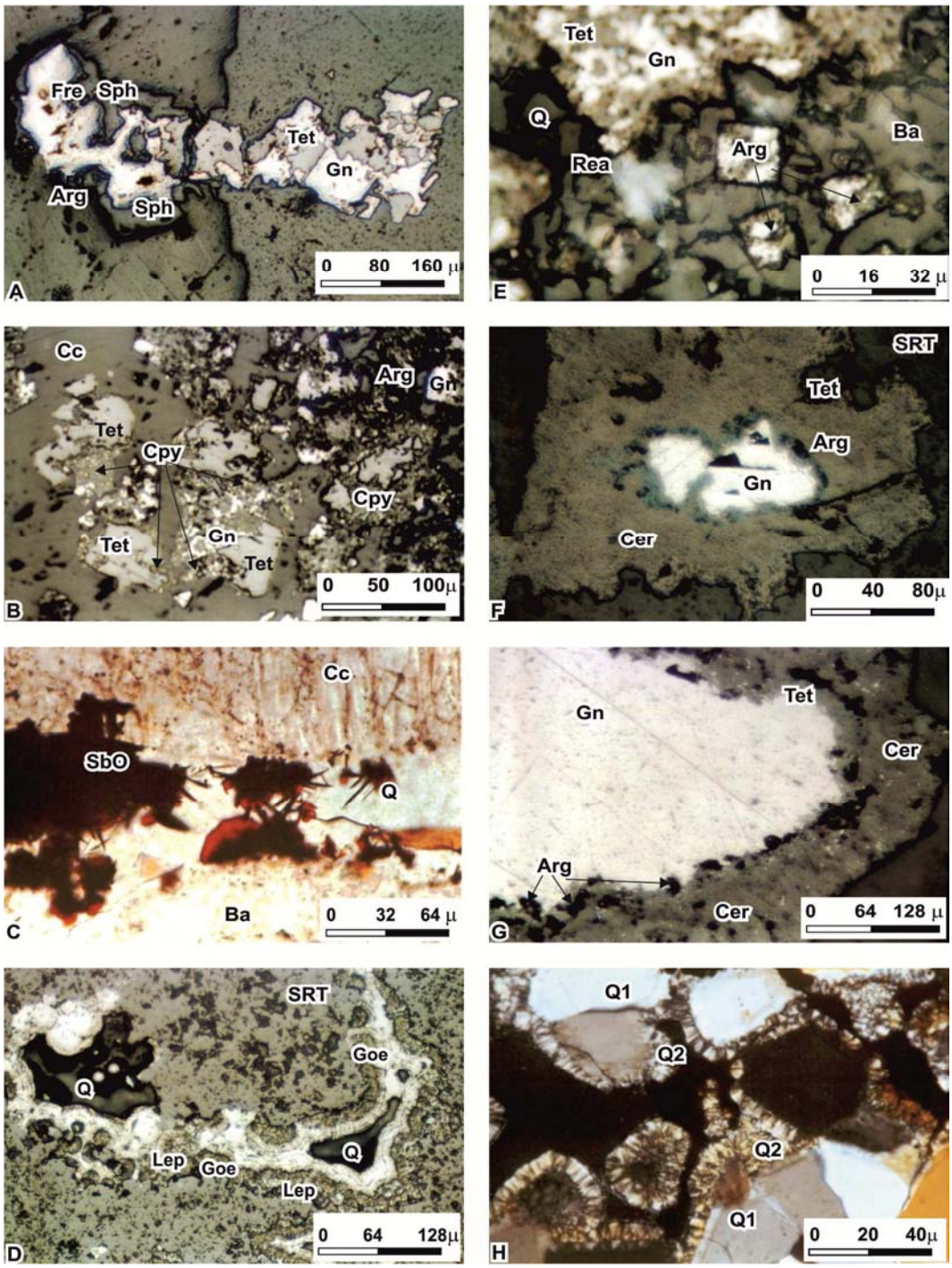

Fig.3. Some ore and gangue minerals in the disseminated and interstice filling type mineralization: (A) Sphalerite (Sp) frameworks replaced by galena (Gn) and cerussite (Cer), tetrahedrite (Tet), freibergite (Fre) and argentite (Arg) in the outer zone of galena (polished section, X nicols), (B) Tetrahedrite (Tet) and argentite (Arg) in the altered zones of galena (Gn) together with altered chalcopyrite (Cpy) in the siliceous limestone (Cc), (polished section, X nicols), (C) Antimony oxides (SbO), calcite (Cc), barite (Ba) and quartz (Q), (thin section //N), (D) Lepydochrocite (Lep), goethite (Goe) and quartz (Q) filling in the interstice of limestone (polished section, //N), (E) Idiomorph argentite (Arg), galena (Gn), tetrahedrite (Tet), barite (Ba) and quartz (Q) in the disseminated type ore (polished section, //N), (F) A galena (Gn) relict, tetrahedrite (Tet) and argentite (Arg) in the cerussite (Cer) (polished section, //N), (G) Altered galena (Gn) and cerussite (Cer), tetrahedrite (Tet) and argentite (Arg) in the altered zone of galena (polished section, //N), (H) Coarse crystallized quartz-1 (Q1) and surrounding quartz-2 (Q2) in the interstices of siliceous rhyodacitic tuffs, (thin section, X nicols).

Table 4. Correlation coefficients of the 25 variables of the rhyolitic and rhyodacitic tuffs of the Tavsanli volcanites (n = 37)

	SiO_2	Al_2O_3	Fe_2O_3	MgO	CaO	Na_2O	K_2O	TiO_2	P_2O_5	MnO	Cr_2O_3	Ni	Cu	Pb	Zn	As	Cd	Sb	Ag	Hg	Tl	Ba	Sr	Zr
SiO_2	1.00	0.36	-0.11	0.15	-0.15	0.36	0.47	0.13	-0.18	0.02	0.16	-0.30	0.21	0.07	-0.11	0.03	-0.05	0.08	0.10	0.22	-0.03	-0.65	-0.60	0.08
Al_2O_3		1.00	-0.16	0.15	-0.02	0.46	0.66	0.62	0.34	-0.12	0.09	0.13	-0.07	-0.05	-0.10	0.10	-0.09	0.18	-0.05	0.16	0.02	-0.27	-0.29	0.45
Fe_2O_3			1.00	-0.01	0.15	-0.16	-0.21	-0.17	0.31	0.53	0.09	0.37	0.00	0.15	0.09	-0.15	-0.17	0.18	0.15	0.08	0.18	0.07	-0.18	-0.01
MgO				1.00	0.52	-0.04	-0.15	-0.03	0.27	0.18	0.05	0.00	-0.05	0.13	0.06	0.33	-0.05	0.21	0.06	-0.02	-0.09	-0.23	-0.25	-0.06
CaO					1.00	0.03	-0.15	-0.13	0.23	0.06	-0.08	0.47	-0.18	0.17	0.05	0.14	-0.05	0.22	0.11	0.07	0.11	0.12	-0.10	0.26
Na_2O						1.00	0.41	0.33	0.03	-0.22	0.10	0.01	-0.03	-0.31	-0.29	-0.01	-0.32	0.02	-0.26	0.12	0.01	-0.07	-0.23	0.40
K_2O							1.00	0.49	-0.28	-0.15	0.16	0.02	0.00	-0.20	-0.22	0.12	-0.03	-0.02	-0.10	0.01	0.09	-0.37	-0.31	0.34
TiO_2								1.00	0.06	-0.22	0.21	0.03	0.10	-0.34	-0.40	0.24	-0.37	-0.05	-0.34	0.05	0.07	-0.25	-0.25	0.55
P_2O_5									1.00	-0.05	-0.08	0.30	-0.14	0.11	0.10	-0.10	-0.11	0.22	0.06	0.08	0.09	0.02	-0.11	0.20
MnO										1.00	0.04	0.01	0.15	0.56	0.51	-0.24	0.30	-0.15	0.47	-0.08	-0.26	0.08	-0.07	-0.15
Cr_2O_3											1.00	-0.02	0.77	-0.04	-0.04	-0.01	-0.11	0.24	0.02	0.58	0.20	0.03	-0.10	0.05
Ni												1.00	-0.10	0.05	0.04	-0.01	-0.05	0.38	0.07	0.22	0.49	0.25	-0.06	0.11
Cu													1.00	0.24	0.25	-0.18	0.19	0.03	0.31	0.36	-0.05	0.02	-0.08	0.10
Pb														1.00	0.80	-0.35	0.73	-0.15	0.89	-0.06	-0.32	0.14	-0.02	0.00
Zn															1.00	-0.28	0.90	-0.13	0.76	-0.07	-0.25	0.28	0.17	-0.19
As																1.00	-0.21	0.41	-0.28	0.22	0.44	-0.32	-0.31	-0.10
Cd																	1.00	-0.18	0.75	-0.14	-0.20	0.20	0.23	-0.20
Sb																		1.00	-0.09	0.65	0.77	-0.05	-0.14	-0.05
Ag																			1.00	0.01	-0.27	0.14	0.03	0.05
Hg																				1.00	0.51	-0.03	-0.20	-0.04
Tl																					1.00	-0.03	-0.17	-0.14
Ba																						1.00	0.71	-0.08
Sr																							1.00	-0.22
Zr																								1.00

with respect to Ag. In addition Cd has strong positive correlation with respect to Ag and, Sb has strong positive correlation with respect to Hg and Tl. Ba has only a positive correlation with respect to Sr (Table 5).

Since ten elements such as Pb, Zn, As, Cd, Sb, Ag, Hg, Tl, Ba and Sr, are directly related to ore deposition, have significant correlations with each other, they were subjected to further statistical analysis (Table 5). Logarithmic histograms of these elements show normal distribution. Simple correlation enabled the determination of relationships between element pairs. The association of the element pairs with very strong positive correlation coefficients is significant in regression analysis. Therefore, interpretations based on the correlation coefficients are meaningful.

In order to understand relationships of the Pb, Zn, As, Cd, Sb, Ag, Hg, Tl, Ba and Sr of ore samples, cluster analysis was utilized by using correlation coefficients. Three significant groups appear in the cluster analysis dendrogram of collected samples (Fig. 4). The first group is represented by the high-temperature trace element group consisting of the Pb-Ag and Zn-Cd pairs, the second group by the low-temperature trace element group, which consists of the Sb-Tl pairs joined with Hg and As and the third group comprising Ba-Sr elements. These groups may form under variable temperature conditions in the epithermal system. Discrimination between the main components and trace

Table 5. Correlation coefficients of the 10 variables of the rhyolitic and rhyodacitic tuffs of the Tavsanli vulcanites (n = 37)

	Pb	Zn	As	Cd	Sb	Ag	Hg	Tl	Ba	Sr
Pb	1.00	0.80	-0.35	0.73	-0.15	0.89	-0.06	-0.32	0.14	-0.02
Zn		1.00	-0.28	0.90	-0.13	0.76	-0.07	-0.25	0.28	0.17
As			1.00	-0.21	0.41	-0.28	0.22	0.44	-0.32	-0.31
Cd				1.00	-0.18	0.75	-0.14	-0.20	0.20	0.23
Sb					1.00	-0.09	0.65	0.77	-0.05	-0.14
Ag						1.00	0.01	-0.27	0.14	0.03
Hg							1.00	0.51	-0.03	-0.20
Tl								1.00	-0.03	-0.17
Ba									1.00	0.71
Sr										1.00

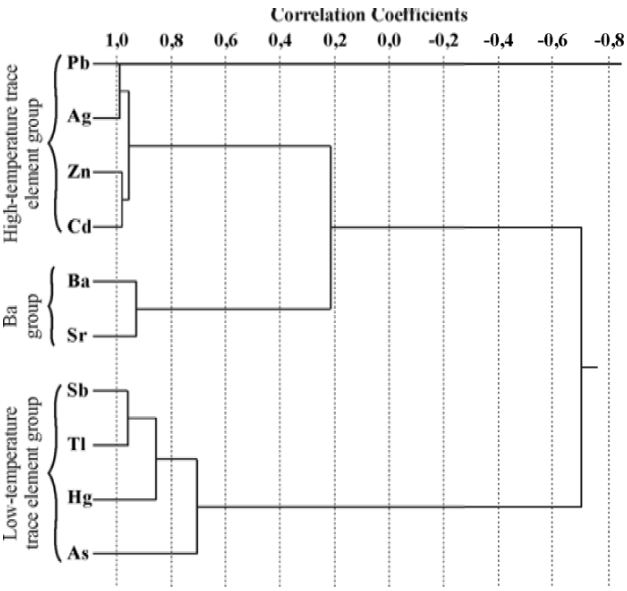

Fig.4. Cluster analysis dendrogram of rhyolitic and rhyodacitic tuffs of the Tavsanli Volcanics with 10 variables.

Table 6. Factor analyse results of first three factor having 10 variables of the analyzed elements of the Tavsanli Volcanites of the Gözeçukuru deposit

Principal ComponentAnalysis			Variance (Extraction Sums of Squared Loadings)			Weights of First 3 Factor			
Component	Extraction	FactorNo	Total	% ofVariance	Cumulative%	Component	Factor1	Factor2	Factor3
Pb	0.89	1	4.00	40.03	40.03	Pb	0.84	0.37	-0.20
Zn	0.88	2	2.22	22.22	62.25	Zn	0.86	0.37	0.01
As	0.46	3	1.64	16.44	78.70	As	-0.56	0.35	-0.17
Cd	0.81	4	0.77	7.71	86.40	Cd	0.83	0.34	-0.01
Sb	0.86	5	0.42	4.18	90.59	Sb	-0.47	0.75	0.28
Ag	0.86	6	0.33	3.33	93.91	Ag	0.81	0.43	-0.16
Hg	0.64	7	0.29	2.87	96.79	Hg	-0.34	0.69	0.20
Tl	0.78	8	0.18	1.76	98.55	Tl	-0.57	0.61	0.30
Ba	0.85	9	0.09	0.93	99.48	Ba	0.37	-0.10	0.84
Sr	0.85	10	0.05	0.52	100.00	Sr	0.34	-0.31	0.80

elements reveals different environments of formation for the epigenetic deposition of ore minerals in the study area. The first group was formed under relatively high temperature conditions, the second under low temperature conditions and the last developed from the residual ore forming solutions.

Factor analysis was intended to show the dependence of structures among grouped variables (Boski and Herbosch, 1990). The recognition of these associations allows for the creation of a small number of hypothetical variables known as factors, with the aim of finding a simple order related with the observed variables. The grouping of major and trace elements, which behave coherently, enables an assesment to be made of the geochemical processes (factors) acting in the paleoenvironment of the study area.

In this study, ten trace elements which have significant correlations with each others, such as, Pb, Zn, As, Cd, Sb, Ag, Hg, Tl, Ba and Sr were used in the factor analysis. R-mode factor analysis of chemical data of the above mentioned 10 elements, including varimax factor rotation of the factor matrix were used in the factor analysis. All of the variables have significant extraction value except As in the principal component analysis. There are three factors with initial eigen values higher than 1 in the factor analysis of ore samples, which represented 78.7% of the total variation (Table 6). Weights of the other 7 factors are very low and thus were neglected in the factor analysis.

The first factor comprises 40.03% of total variation and is represented by significant positive weights of Pb, Zn, Cd and Ag and significant negative weights of As, Sb, Hg and Tl (Table 6; Fig. 5). In the distribution of elements having positive and negative weights, the positive weights are equivalent to the high-temperature trace element group of cluster analysis and the negative weights are equivalent to the low-temperature trace element groups of cluster analysis. Positive factor weights of Pb, Zn, Cd and Ag reflect the formation of primary sulphide minerals of these elements such as galena, sphalerite and argentite at the early stage of primary ore deposition in the Gözeçukuru Mine. Negative factor weights of the As, Sb, Hg and Tl indicate that these elements behaved similarly at the later stages of mineralization.

The second factor has 22.22% of total variation and is represented by significant positive weights of Sb, Hg and Tl, lower negative factor weights of Sr and less important positive weights of Pb, Zn, As, Cd and Ag. When compared with the cluster analysis, Sb, Hg and Tl that have positive weights of the second factor coincide with low temperature trace element group (Fig. 5). Second factor shows the formation of the sulphide and sulphosalt minerals under the relatively low-temperature conditions at the later stages of ore depositions. These minerals are mainly antimonite

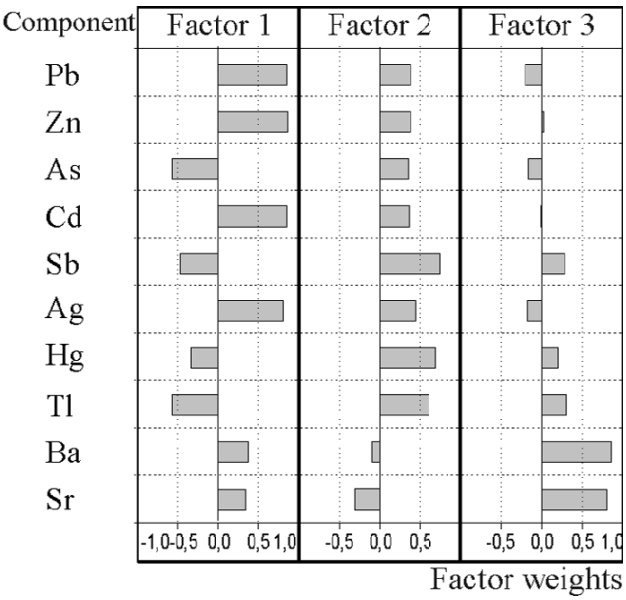

Fig.5. Factor weights of the analyzed components of first 3 factor in the Gözeçukuru As-Sb deposit.

(Sb_2S_3), realgar (As_2S_3), orpiment (AsS) tetrahedrite $(Cu,Fe,Zn,Ag)_{12}Sb_4S_3$, and minor amounts tennantite $(Cu,Fe,Zn,Ag)_{12}As_4S_3$, pyrargyrite ($Ag_3SbS_3$), praustite ($Ag_3AsS_3$), pyrostilpnite $(Ag,Cu,Fe)_3SbS_3$), stephanite (Ag_5SbS_4) andorite ($PbAgSb_3S_6$), cinnabar (HgS), enargite (Cu_3AsS_4), boulangerite $[(Pb,Ag)_{2-5}Sb_{2-4}S_{5-11}]$ and bournonite $[(Pb,Cu,Ag)_2SbS_3]$. Some of these minerals formed at the early to late stages of mineralization.

The third factor has 16.44% of total variation and is represented by significant positive factor weights of Ba and Sr and coincides with the Ba group of cluster analysis (Figs. 4 and 5). This factor represents interstices-filling mineralization type when barite as a gangue mineral was precipitated during the late phase of mineralization in the rhyolitic and rhyodacitic tuffs. Significant Sr weight depends on the relationship between the Ba and Sr in the geochemical environment.

Factor analyses indicate mineralization stages of the Gözeçukuru As-Sb-Pb-Zn deposits. The first factor shows primary sulphide mineralization at high-temperatures in the early stages of mineralization. The second factor indicates formation of sulphide and sulphosalts at low-temperature. The last factor indicates filling of interstices type mineralization and cyrstallization of barite.

Fluid inclusion studies of barite collected in the study area gave information about the physical and chemical characteristics of the environment of mineral precipitation.

The fluid inclusion data of the Gözeçukuru deposit shows two formation stages (Arik, 2002). Micrometric measurement of a barite sample from a barite vein, within, the rhyolitic tuffs has primary and secondary monophase liquid and bi-phase (liquid plus vapor) liquid inclusions. Dimensions of the primary liquid inclusions are 2–80 μm, and the void-filling ratio is 30–70%. Homogenization temperature measurements were performed on the 23 primary bi-phase fluid inclusion of the barite samples which range from 170 to 300 ºC. The average homogenization temperature of the primary and bi-phase inclusions is 221 °C, and the average homogenization temperature of the secondary and bi-phase inclusion is 60–80 °C (Arik, 2002). Liquid inclusion studies by Vicil (1982) from the Aktepe silver deposit show that homogenization temperatures of liquid inclusions range from 137 to 233 °C for barite in the barite-galena veins, 110–115 °C for barite accompanying chalcedony and 120–230 °C for barite in the barite-stibnite veins. All the homogenization temperatures of barite indicated medium- and low-temperature hydrothermal fluids. Therefore, ore deposition in the study area took place in the epithermal stage of the hydrothermal system.

CONCLUSIONS

Genetic characterizations of the mineralization based on the geological, mineralogical and geochemical studies on the Gözeçukuru As-Sb deposit are given below.

1. Pb, Zn, As, Sb, Ag and Ba enrichments in the study area took place principaly in the rhyodacitic and rhyolitic tuffs of the middle to upper Miocene Tavsanli volcanics with minor amounts, within, the Carboniferous–Permian low grade metamorphic rocks of the Sahin Formation and in the limestone and dolomitic limestone of the Pliocene Emet Formation.
2. According to mineral paragenesis, crystallization structure, location and dispersion in the wall rock, the mineralizations were classified into three different geometries: vein, dissemination and interstice-filling.
3. Mineralization formed in two stages, the first being the principal mineralization, and the second being post–principal mineralization. Pb, Zn, Sb and As enrichment occurred during both stages. Sphalerite, galena, stibnite and realgar were formed during the hydrothermal stage of magmatic mineralization rather than under other conditions. The mineral paragenesis, stratigraphical position, epigenetic texture and structures of mineralization such as vein and interstices- filling and fluid inclusion data indicate the epigenetic ore deposition.
4. The many positive correlation coefficients among Pb, Zn, As, Sb, Cd, Hg, Tl, Ba and Sr in the multivariate analysis indicate that these elements were mobilized together during mineralization.
5. Three significant groups appear in the cluster analysis dendrogram of rhyolitic and rhyodacitic tuff samples. The first group is represented by the high-temperature trace element group comprising of Pb-Ag and Zn-Cd pairs. The second the low-temperature trace element group, consists of Sb-Tl pairs joined by Hg and As, and the third group by Ba-Sr elements.
6. Factor analysis supports element discrimination by cluster analysis. Three significant factors were identified in the factor analysis. First factor typifies primary sulphide deposition, second factor depicts the formation of the low-temperature sulphide and sulphosalt minerals and the last factor represents the barite formation in the interstices of the wall-rocks.
7. Homogenization temperatures of fluid inclusions show a range of formation temperatures of mineralization from 221 °C to 60 °C. These temperature ranges coincide with primary and secondary mineralization.

All these data provide a rather complete picture of the mineralization of the Gözeçukuru As-Sb deposit which took place under epithermal conditions during the Miocene and Pliocene Epochs. After ore deposition, the mineralized zone was tectonically uplifted, allowing extensive surface weathering.

Acknowledgments: This study was supported by Selçuk University Coordinatories of Scientific Research with SU-BAP 08-701110 project numbers. A part of the data also was obtained under 2007/07201033 project number. The author thanks the Principal of Selçuk University and the Coordinators of Scientific Research of Selçuk University, Prof. Dr. Hükmü Orhan from Selçuk University Geological Engineering Department (Turkey), Prof. Dr. Simon Pirc from Univesity of Ljulbjana (Slovenia).

References

Akyol, Z. (1975) Observation of barite appearence of Tavsanli–Dudas. Bull. General Directory of Mineral Research and Exploration Institute of Turkey, v.85, pp.161-172.

Arik, F. (2002) Geochemical modelling of Gümüsköy (Kütahya) silver deposit; University of Selçuk, Institute of the Natural and Applied Sciences, Ph.D. Dissertation Thesis, Konya, 318p.

Arik, F. (2008) Geological, petrographical and geochemical characteristics of Sigiregregi (Sahin–Kütahya) Zn-Pb ore deposit; Symposium on geology, mining and present problems of lead-zinc deposits of Türkiye; Istanbul University, Department of Geological and Mining Engineering, 154–183.

Arik, F. and Temur, S. (2003) Stratigraphy of the Köprüören–Gümüþköy–Yoncali (Kütahya) District. Bull. Engineering-Architecture Faculty of Selçuk University, Konya (in Turkish), v.18, pp.21-36.

Arik, F. and Nalbantçilar M.T. (2004) The negative effect of ore deposits of the west of Kütahya on surface and ground water; 57th General Assemblages of Geology, United Chambers of Engineering and Architects of Turkey, Chamber of Geology Engineers, Extended Abstracts, pp.261-262.

Arik, F., Yaldiz, T. and Bozkir, Y. (2008) Geological, petrographical and geochemical characteristics of Aktepe (Gümüsköy-Kütahya) Zn-Pb-Ag ore deposit, Syposium on geology, mining and present problems of lead-zinc deposits of Türkiye; Istanbul University, Department of Geological and Mining Engineering, pp.119-153.

Bas, H. (1986) Tertiary geology of Domaniç–Tavsanli–Kütahya–Gediz districts; Bulletin of Geology Engineering, United Chambers of Engineering and Architects of Turkey, Society of Geology Engineers, v.27, pp.11-18.

Bas, H. (1987) Characteristics of Tavsanli-Domaniç (Kütahya) volcanics and importance on the Senozoic volcanism of West Anatolia; Bulletin of Geology Engineering, United Chambers of Engineering and Architects of Turkey, Society of Geology Engineers (In Turkish), v.30, pp.67-80.

Boski, T. and Herbosch, A. (1990) Trace elements and their relation to the mineral phases in the lateritic bauxites from Southeastern Guinea, Bissau. Chem. Geol., v.82, pp.279-297.

Çelik Y. and Kerey Ý.E. (1999) Lithofacies and deposition environments of coal bearing sediments of Domaniç Neogene Basin; 52th Geological Congress of Türkiye, United Chambers of Engineering and Architects of Turkey, Society of Geology Engineers, Ankara, papers, pp.318-325.

Ercan, T. (1979) Cenozoic volcanism of West Anatolia, Trakia and Aegean Islands; Geological Engineering, United Chambers of Engineering and Architects of Turkey, Society of Geology Engineers, v.9, pp.23-46.

Ercan, T. (1982) Young tectonics and volcanism of West Anatolia; United Chambers of Engineering and Architects of Turkey, Society of Geology Engineers, Board of Young Tectonics and Volcanism of West Anatolia. *In:* O. Erol and V. Oygür (Eds.), General Directorate of Mineral Research and Exploration Institute of Turkey, pp.5–14.

Ercan, T., Satir, M., Kreuzer, H., Türkecan, A., Günay, E., Çevikbas, A., Ates, M. and Can, B. (1985) Interpretation of new chemical, isotopic, and radiometric data of Senozoic volcanics in the West Anatolia; Bulletin of Geology Engineering, United Chambers of Engineering and Architects of Turkey, Society of Geology Engineers, v.28, pp.121-136.

Erdogan, E. (1971) Etude of the Yoncali (Kütahya) Hot Spring; General Directorate of Mineral Research and Exploration Institute of Turkey, Report no. 2244, 29p.

Gümüs, A. (1998) Ore Geology, Geological Prospection and Reservoir Calculations (1st print.); Bilim Ofsset, Izmir, 400p.

Gün, H., Akdeniz, N. and Günay, E. (1979) Geology and age problems of Neogene basins south of Gediz and Emet; Bulletin of Geology Engineering, United Chambers of Engineering and Architects of Turkey, Society of Geology Engineers, v.8, pp.3–13.

Ildiz, T. (1967) Preliminary report of lead districts, authorization numbers 568 and 137, of Kütahya–Gümüsköy; General Directorate of Mineral Research and Exploration Institute of Turkey, Compilation Report no.435 (270), 5p.

Kafkas, M.A. (1994) Geology and mineralogy of the Aktepe Silver deposits. Directorate of Etibank 100th Year Silver Ore Production Establishment, Kütahya, Brief Report 12p.

Karabas, A. (1997) Geology and genesis of the Gümüsköy (Kütahya) silver deposits; Selçuk Üniversity, Engineering Architecture Faculty, 20th Year Geology Symposium, Communications, pp.229-304.

Sengüler, I. and Sonel, N. (1999) Stratigraphic features and economically impotance of the Seyitömer (Kütahya) bituminous marls; 52th Geology Symposium of Turkey, United Chambers of Engineering and Architects of Turkey, Society

of Geology Engineers (in Turkish), v.30, pp.67-80.

Ünsal, A. and Koçak N. (1981) Preliminary Report of Complex Kütahya–Gümüsköy Ag-Pb-Zn-Sb-$BaSO_4$ Ore Deposit, Presidency of Mining Exploration Department of General Directorate of ETIBANK, 213p.

Vicil, M. (1982) Mineralization of Gümüsköy (Kütahya) Aktepe Pb–Zn–Sb–Ag; Aegean University, Faculty of Geology, Ph.D. Dissertation Thesis, Izmir, 258 pp.

Yaldiz, T. (2007) Mineral enrichments effects to public health located among the Aliköy, Vakif and Köreken (Tavºanli-Kütahya) villages; University of Selçuk, Institute of the Natural and Applied Sciences, M.Sc. Thesis, 114p.

Yigitgüden, H.Y. (1984) Silver ore deposit located vicinity of Kütahya West Anatolia–Türkiye; Rainland Westfalen Technical High School, Mining and Metallurgy Faculty, Ph.D. Dissertation Thesis, 192p.

Ziegler J. (1960) Brief report on the barite-graphite ores vicinity of Gümüsköy–Kütahya, General Directorate of Mineral Research and Exploration Institute of Turkey, Comp. Rep. no. 448 (In Turkish), 7 pp. General Directorate of Mineral Research and Exploration Institute of Turkey, pp.5–14.

(Received: 25 May 2009; Revised form accepted: 23 February 2012)